International Journal of Applied Mathematics

Volume 35 No. 4 2022, 515-528
ISSN: 1311-1728 (printed version); ISSN: 1314-8060 (on-line version)
doi: http://dx.doi.org/10.12732/ijam.v35i4.2

NON OSCILLATORY CENTRAL SCHEMES FOR GENERAL NON-LOCAL TRAFFIC FLOW MODELS

Said Belkadi[1] §, Mohamed Atounti[2]

[1,2] Mohammed First University-Oujda
Polydisciplinary Faculty of Nador, MOROCCO

Abstract: In this research paper, we present a second order non-oscillatory central scheme. Our aim is to solve a non-local conservation law arising in traffic flow models with non-local mean velocity. The proposed scheme proves to be more accurate. It, in some way, resembles the Godunov-type scheme. Yet, it is better than the widely used Lax-Friedrich-type scheme. To prove our thesis, We conduct a series of numerical experiments in which we perform the following: A) We study and test the ratio of accuracy of our second-order scheme. B) We make clear and demonstrate the non-oscillatory character. C) We examine the convergence of the non-local solution to the local solution.

AMS Subject Classification: 35L65, 65M08, 90B20
Key Words: finite volume method; non-local conservation laws; traffic flow models

1. Introduction

The first aim of this study is to present the class of non-local conservation laws for traffic flow introduced in [10], where instead of a mean downstream density another mean velocity is considered. More precisely, we consider the following mass conservation equation for traffic with non-local flux of the form.

$$\partial_t \rho + \partial_x (f(\rho)(\kappa_\eta * v(\rho))) = 0, \quad x \in \mathbb{R}, t > 0, \tag{1}$$

Received: August 29, 2021

§Correspondence author

where

$$\kappa_\eta * v(\rho)(t,x) = \int_x^{x+\eta} \kappa_\eta(y-x)v(\rho(t,y))dy, \quad \eta > 0,$$

$\rho(t,x)$ is the unknown density while the convolution kernel κ_η is a non increasing function such that $\kappa_\eta \in C^1([0,\eta];\mathbb{R}^+)$ and $\int_0^\eta \kappa_\eta(x)dx = 1$. We consider the general non-increasing velocity function $v \in C^2([0,\rho_{\max}];\mathbb{R}^+)$ and f is a function such that $f \in C^1([0,\rho_{\max}],\mathbb{R})$, where $\rho_{\max}$ denotes the maximal density.

We set the convolution product as follows:

$$U(t,x) = \kappa_\eta * v(\rho)(t,x),$$

and the flux:

$$F(\rho,U) = f(\rho)U.$$

Therefore, we rewrite (1) as:

$$\partial_t\rho(t,x) + \partial_x F\left(\rho, U(t,x)\right) = 0, \quad x \in \mathbb{R},\, t > 0,$$

with the following initial data

$$\rho(0,x) = \rho_0(x) \in BV\left(\mathbb{R},[0,\rho_{\max}]\right). \tag{2}$$

Notice: In [6, 10], the well-posedness of this model was considered, as well as the creation of a first-order FV approximation.

These non-local conservation laws equations, which appear in several models such as: sedimentation [3], pedesterian [5, 7] and vehicula [10, 6, 11, 4], are based on the integration of the speed which depends on the function that represents the density of agents (cars, pedesterians). We assume that drivers adapt their speed based on a mean downstream velocity, see [10]. Yet, over recent years, several analytical results on non-local conservation laws were conducted (we refer to[17] for scalar equations in one space dimension, [1, 7, 14, 13] for scalar equations in several space dimensions and [8] for multi-dimensional systems of conservation laws). However, few specific numerical methods have been developed up till now. To our knowledge, two main approaches have been proposed to treat non-local problems: Lax-Friedrich's first and second order central schemes and Nassyau-Tadmor's [12, 1, 3, 7]. The study of the model for traffic flow in one space dimensions, which is presented in [10], encourages the use of second order central schemes (SCS) due to their versatility and lower computational costs. In addition, the computation process induced by the presence of discontinuities at each interface, which require the resolution of Riemann's problems at each time step, motivates the need to develop high order algorithms.

This paper is organized according to the following structures: In Section 2, we review a simple first order Finite volume schemes. In Section 3, we present the details for increasing the order of approximation by using the MUSCL-approach. In Section 4, we present numerical applications that demonstrate the interest of the proposed approach. In Section 5, we finally summarize the results and provide a conclusion.

2. A review of Finite Volume schemes for non-local conservation laws

For the sake of simplicity, we divide the computational domain into cells $[x_{j-\frac{1}{2}}, x_{j+\frac{1}{2}}]_{j\in\mathbb{Z}}$ of a uniform size Δx with $x_j = j\Delta x$ and $x_{j+\frac{1}{2}} = (j+\frac{1}{2})\Delta x$. Let us denote by ρ_j^0 the approximation of the average of the initial datum

$$\rho_j^0 = \frac{1}{\Delta x}\int_{x_{j-\frac{1}{2}}}^{x_{j+\frac{1}{2}}} \rho(0,x)dx$$

and denote by ρ_j^n the approximation of the average of the exact solution at j^{th} cell, $[x_{j-\frac{1}{2}}, x_{j+\frac{1}{2}}]$ at time level t^n,

$$\rho_j^n = \frac{1}{\Delta x}\int_{x_{j-\frac{1}{2}}}^{x_{j+\frac{1}{2}}} \rho(t^n,x)dx.$$

These cell averages are combined to form the piecewise constant function

$$\rho_{\Delta x}(t^n,x) = \rho_j^n, \quad (t,x) \in [t^n, t^{n+1}[\times[x_{j-\frac{1}{2}}, x_{j+\frac{1}{2}}].$$

We compute the cell average at the next time level by integrating the nonlocal conservation law (1) over the domain $[t^n, t^{n+1}[\times [x_{j-\frac{1}{2}}, x_{j+\frac{1}{2}}]$. This gives

$$\int_{x_{j-\frac{1}{2}}}^{x_{j+\frac{1}{2}}} \rho(t^{n+1},x)dx = \int_{x_{j-\frac{1}{2}}}^{x_{j+\frac{1}{2}}} \rho(t^n,x)dx$$
$$-\int_{t^n}^{t^{n+1}} F(\rho(t,x_{j+\frac{1}{2}},U(t,x_{j+\frac{1}{2}}))dt + \int_{t^n}^{t^{n+1}} F(\rho(t,x_{j-\frac{1}{2}}),U(t,x_{j-\frac{1}{2}}))dt. \quad (3)$$

Defining

$$F_{j+\frac{1}{2}}^n = \frac{1}{\Delta t}\int_{t^n}^{t^{n+1}} F(\rho(t,x_{j+\frac{1}{2}}),U(t,x_{j+\frac{1}{2}}))dt.$$

And, dividing both sides of (3) by Δx, we obtain

$$\rho_j^{n+1} = \rho_j^n - \lambda(F^n_{j+\frac{1}{2}} - F^n_{j-\frac{1}{2}}), \quad \lambda = \frac{\Delta t}{\Delta x}, \tag{4}$$

where $F_{j+\frac{1}{2}}$ is defined using a standard consistent numerical flux at each interface $x_{j+\frac{1}{2}}$.

The choice of intercell flux $F_{j+\frac{1}{2}}$ in (4) determines the particular numerical scheme for equation (1).

2.1. Godunov-type scheme

To define a Godunov scheme for the nonlocal equation (1) we first compute the convolution term

$$\begin{aligned} U^n_{j+\frac{1}{2}} &= \int_{x_{j+\frac{1}{2}}}^{x_{j+\frac{1}{2}}+\eta} \kappa_\eta \left(y - x_{j+\frac{1}{2}}\right) v\left(\rho\left(t,y\right)\right) dy \\ &= \sum_{k=1}^{k=N} \int_{x_{j+k-\frac{1}{2}}}^{x_{j+k+\frac{1}{2}}} \kappa_\eta \left(y - x_{j+\frac{1}{2}}\right) v\left(\rho\left(t,y\right)\right) dy \\ &= \sum_{k=1}^{k=N} \mu_k v\left(\rho^n_{j+k}\right), \end{aligned}$$

where $\mu_k = \int_{x_{k-1}}^{x_k} \kappa_\eta\left(x\right) dx$.

The numerical flux function of the Godunov scheme is given by:

$$F^n_{j+\frac{1}{2}} = U^n_{j+\frac{1}{2}} f(\rho^n_j). \tag{5}$$

Hence, the Godunov scheme is (4) with the Godunov flux (5), we refer to [10] for more details.

2.2. Lax-Friedrich-type scheme

The numerical flux of LxF scheme adapted to (1) is given by:

$$F^n_{j+\frac{1}{2}} = \frac{V^n_j f(\rho^n_j) + V^n_{j+1} f(\rho^n_{j+1})}{2} + \frac{\alpha}{2}(\rho^n_j - \rho^n_{j+1}) \tag{6}$$

with $\alpha \geqslant 0$ being the viscosity coefficient, where the V^n_j is the downstream velocity rate of the convolution term computed by:

$$V^n_j = v\left(\Delta x \sum_{k=0}^{N-1} \kappa_\eta(k\Delta x)\rho^n_{j+k}\right).$$

Hence, the Lax-Friedrich scheme is (4) with the modified Lax-Friedrich flux (6), we refer to [6, 11] for more details.

In [10], the authors prove that the Godunov-type scheme is more accurate than the Lax-Friedrich scheme for this model (1). The Godunov scheme is subject to lower numerical viscosity, but it requires a Riemann solver for its numerical constructions. The Lax-Friedrich scheme is the forerunner of all central schemes. Unfortunately, the excessive numerical viscosity in the Lax-Friedrich scheme gives a relatively poor solution. To increase the order of accuracy, we propose a scheme of the second order of accuracy, which is better than the Lax-Friedrich scheme according to the achieved results. This scheme retains the advantage of a simple recipe, works without a Riemann solver, and gives simultaneous high resolution if compared to the results of Godunov's and Lax-Friedrich results.

3. Second order non-oscillatory central schemes

In this section, we propose a second-order resolution approximation of (1), which is based on the staggered form of the Lax-Friedrich (LxF) scheme [9, 12],

$$\rho_{j+\frac{1}{2}} = \frac{1}{2}(\rho_j + \rho_{j+1}) - \lambda \left(F(\rho_{j+1}, U_{j+1}) - F(\rho_j, U_j)\right).$$

We follow a predictor-corrector approach like the MUSCL-type scheme that was introduced by Van Leer. The main aim is to modify the piecewise constant ρ_j^n by the piecewise linear functions, [15, 16]. More specifically, at each (time level t^n), we reconstruct a piecewise linear approximation of the form:

$$\tilde{\rho}^n(x) = \rho_j^n + \sigma_j(x - x_j), \quad x \in [x_{j-\frac{1}{2}}, x_{j+\frac{1}{2}}]. \tag{7}$$

This form retains conservation, i.e.,

$$\frac{1}{\Delta x}\int_{x_{j-\frac{1}{2}}}^{x_{j+\frac{1}{2}}} \tilde{\rho}^n(x)dx = \rho_j^n.$$

Hence, the second-order accuracy is guaranteed if the vector of an approximate slope at the grid point x_j, σ_j, satisfies

$$\sigma_j = \Delta x \frac{\partial \rho}{\partial x}(t, x = x_j) + o((\Delta x)^2).$$

To ensure a non-oscillatory nature of reconstruction and thus avoid spurious oscillations in the numerical solution, we have to evaluate σ_j^n using a nonlinear limiter. In our numerical tests, we use a generalized minmod limiter:

$$\sigma_j^n = mm\left(\theta mm\left(\frac{\rho_j^n - \rho_{j-1}^n}{\Delta x}, \frac{\rho_{j+1}^n - \rho_j^n}{\Delta x}\right), \frac{\rho_{j+1}^n - \rho_{j-1}^n}{2\Delta x}\right),\ \theta \in [1,2], \tag{8}$$

where the minmod function (denoted as mm) is defined as

$$\mathrm{mm}(a,b) = \frac{1}{2}(\mathrm{sign}(a) + \mathrm{sign}(b)).\min(|a|,|b|),$$

for two scalars (a) and (b) (the sign denotes the sign function) and the parameter θ can be used to control the amount of numerical viscosity present in the resulting scheme.

Next, we evolve the piecewise linear function (7) by integrating the (1) over the domain $[t^n, t^{n+1}] \times [x_j, x_{j+1}]$. We get:

$$\begin{aligned}\frac{1}{\Delta x}\int_{x_j}^{x_{j+1}} \rho(t^{n+1},x)dx = \frac{1}{\Delta x}\int_{x_j}^{x_{j+1}} \rho(t^n,x)dx \\ - \frac{1}{\Delta x}\left(\int_{t^n}^{t^{n+1}} F\left(\rho(t,x_{j+1}), U(t,x_{j+1})\right)dt\right) \\ + \frac{1}{\Delta x}\left(\int_{t^n}^{t^{n+1}} F\left(\rho(t,x_j), U(t,x_j)\right)dt\right).\end{aligned} \tag{9}$$

Defining

$$\rho_{j+\frac{1}{2}}^n = \frac{1}{\Delta x}\int_{x_j}^{x_{j+1}} \rho(t^n,x)dx.$$

The staggered averages, $\rho_{j+\frac{1}{2}}^n$ can be computed exactly as

$$\begin{aligned}\rho_{j+\frac{1}{2}}^n &= \frac{1}{\Delta x}\int_{x_j}^{x_{j+1}} \tilde{\rho}(t^n,x)dx \\ &= \frac{\rho_j^n + \rho_{j+1}^n}{2} + \frac{\Delta x}{8}\left(\sigma_j - \sigma_{j+1}\right).\end{aligned}$$

The resulting central scheme (9) then is written as follows:

$$\rho_{j+\frac{1}{2}}^{n+1} = \frac{\rho_j^n + \rho_{j+1}^n}{2} + \frac{\Delta x}{8}\left(\sigma_j - \sigma_{j+1}\right)$$

$$- \frac{1}{\Delta x}\left(\int_{t^n}^{t^{n+1}} F\left(\rho(t,x_{j+1}),U(t,x_{j+1})\right)dt\right) + \frac{1}{\Delta x}\left(\int_{t^n}^{t^{n+1}} F\left(\rho(t,x_j),U(t,x_j)\right)dt\right). \quad (10)$$

Within (10), if the CFL condition is:

$$\lambda < \frac{1}{2\lambda_{\max}}, \quad \lambda_{\max} := \max_{\rho\in[\rho_{\min},\rho_{\max}]}\left|\frac{dF(\rho,U)}{d\rho}\right|.$$

It is then fulfilled, and the numerical flux is approximated by the second-order midpoint rule. We have

$$\int_{t^n}^{t^{n+1}} F\left(\rho(t,x_j),U(t,x_j)\right)dt \simeq \Delta t F(\rho(t^{n+\frac{1}{2}},x_j),U(t^{n+\frac{1}{2}},x_j))dt. \quad (11)$$

And, according to Taylor's expansion and the nonlocal conservation law (1), the pointwise values at the half-time steps are methodically evaluated as follows:

$$\begin{aligned}\rho(t^{n+\frac{1}{2}},x_j) &\simeq \rho(t^n,x_j)+\tfrac{\Delta t}{2}\rho_t(t^n,x_j)\\ &= \rho_j^n - \tfrac{\lambda}{2}F_j',\end{aligned} \quad (12)$$

where $\frac{1}{\Delta x}F_j' = \partial_x F\left(\rho(t,x=x_j),U(t,x=x_j)\right)+O(\Delta x)$, and

$$U(t^{n+\frac{1}{2}},x_j) \simeq U(t^n,x_j)+\frac{\Delta t}{2}U_t(t^n,x_j). \quad (13)$$

The space derivative F_j' is approximated by the minmod limiters

$$F_j' = mm\left(\theta\times mm\left(\frac{F_j^n-F_{j-1}^n}{\Delta x},\frac{F_{j+1}^n-F_j^n}{\Delta x}\right),\frac{F_{j+1}^n-F_{j-1}^n}{2\Delta x}\right),$$

where (F_j denote $F(\rho_j,U_j)$.

We compute the terms in (14) by the mid-point and the composite trapezoidal rules. We get:

$$\begin{aligned}U\left(t^n,x_j\right) &= \int_{x_j}^{x_j+\eta} v\left(\rho\left(t^n,y\right)\right)\kappa_\eta\left(y-x_j\right)dy\\ &\approx \int_{x_j}^{x_{j+\frac{1}{2}}} v(\tilde{\rho}^n(y))\kappa_\eta(y-x_j)dy + \int_{x_{j+N-\frac{1}{2}}}^{x_{j+N}} v(\tilde{\rho}^n(y))\kappa_\eta(y-x_j)dy\end{aligned}$$

$$
\begin{aligned}
&+\sum_{k=1}^{N-1}\int_{x_{j+k-\frac{1}{2}}}^{x_{j+k+\frac{1}{2}}} v(\tilde{\rho}^n(y))\kappa_\eta(y-x_j)dy\\
&=\left[\kappa_\eta(0)v(\rho_j^n)+\kappa_\eta(\frac{\Delta x}{2})v(\rho_j^n+\sigma_j\frac{\Delta x}{2})\right]\frac{\Delta x}{4}\\
&+\left[\kappa_\eta(x_N)v(\rho_{j+N}^n)+\kappa_\eta(x_{N-\frac{1}{2}})v\left(\rho_{j+N}^n-\sigma_{j+N}\frac{\Delta x}{2}\right)\right]\frac{\Delta x}{4}\\
&+\sum_{k=1}^{N-1}\Delta x\kappa_\eta(k\Delta x)v(\rho_{j+k}^n),
\end{aligned}
$$

and

$$
\begin{aligned}
U_t\left(t^n,x_j\right)&=\int_{x_j}^{x_j+\eta} v'\left(\rho\left(t^n,y\right)\right)\rho_t\left(t^n,y\right)\kappa_\eta\left(y-x_j\right)dy\\
&=-\int_{x_j}^{x_j+\eta} v'(\rho(t^n,y))F_y\left(\rho(t^n,y),U(t^n,y)\right)\kappa_\eta(y-x_j)dy\\
&=-\left[v'\left(\rho\left(t^n,y\right)\right)\kappa_\eta\left(y-x_j\right)F\left(\rho\left(t^n,y\right),U(t^n,y)\right)\right]_{x_j}^{x_j+\eta}\\
&\quad+\int_{x_j}^{x_j+\eta}\left(v'(\rho(t^n,y))\kappa_\eta(y-x_j)\right)'F\left(\rho(t^n,y),U(t^n,y)\right)dy\\
&=v'\left(\rho_j^n\right)\kappa_\eta\left(0\right)F\left(\rho_j^n,U_j^n\right)-v'\left(\rho_{j+N}^n\right)\kappa_\eta\left(x_N\right)F\left(\rho_{j+N}^n,U_{j+N}^n\right)\\
&\quad+\frac{\Delta x}{2}\left(v'\left(\rho_j^n\right)\kappa_\eta'\left(0\right)+v''\left(\rho_j^n\right)\sigma_j\kappa_\eta\left(0\right)\right)F\left(\rho_j^n,U_j^n\right)\\
&\quad+\frac{\Delta x}{2}v'\left(\rho_{j+N}^n\right)\kappa_\eta'\left(\eta\right)F\left(\rho_{j+N}^n,U_{j+N}^n\right)\\
&\quad+\frac{\Delta x}{2}v''\left(\rho_{j+N}^n\right)\sigma_{j+N}\kappa_\eta\left(\eta\right)F\left(\rho_{j+N}^n,U_{j+N}^n\right)\\
&\quad+\Delta x\sum_{k=1}^{N-1}v'\left(\rho_{j+k}^n\right)\kappa_\eta'\left(x_k\right)F\left(\rho_{j+k}^n,U_{j+k}^n\right)\\
&\quad+\Delta x\sum_{k=1}^{N-1}v''\left(\rho_{j+k}^n\right)\sigma_{j+k}\kappa_\eta\left(x_k\right)F\left(\rho_{j+k}^n,U_{j+k}^n\right).
\end{aligned}
$$

To sum up the things said, let us formulate the following predictor-corrector scheme:

Step 1: The first step is to predict the solution at half time level:

$$
\rho_j^{n+\frac{1}{2}}=\rho_j^n+\frac{\Delta t}{2}F_j' \tag{14}
$$

$$U_j^{n+\frac{1}{2}} = U_j^n + \frac{\Delta t}{2} U_t(t^n, x_j). \tag{15}$$

Step 2: The second step uses the predicted solution at half time level to update the solution to next time level:

$$\rho_{j+\frac{1}{2}}^{n+1} = \frac{\rho_j^n + \rho_{j+1}^n}{2} + \frac{\Delta x}{8}(\sigma_j - \sigma_{j+1}) - \lambda \left(F(\rho_{j+1}^{n+\frac{1}{2}}, U_{j+1}^{n+\frac{1}{2}}) - F(\rho_j^{n+\frac{1}{2}}, U_j^{n+\frac{1}{2}}) \right). \tag{16}$$

4. Numerical tests

In this section, we perform several test cases with the aim of illustrating the performance of the non-oscillatory-central schemes that were proposed in the previous section (3) in order to prove the numerical approximation of solutions on a bounded interval that is $I = [-1, 1]$. In all our numerical tests, we employ linear velocity: $v(\rho) = 1-\rho$, $f(\rho) = \rho$, and we use periodic boundary conditions for simplicity. Let us divide the domain $[-1, 1]$ into cells of size $\Delta x = \frac{2}{m}$ such that $\eta = N\Delta x$ for some $N \in \mathbb{N}$ besides. In order to compute the numerical fluxes $F_{j+\frac{1}{2}}$ for $j = 0, \ldots, m+1$, we define ρ_j^n in the ghost cells as follows:

$$\rho_0^n = \rho_m^n, \quad \rho_{m+j}^n = \rho_j^n \ \text{ for } j = 1, \ldots, N.$$

Test 1: We compute the numerical solution of (1)-(2) at time, $T = 0.63$ with $\eta = 0.1$, $\kappa_\eta(x) = \frac{2}{\eta}(1 - \frac{x}{\eta})$ and $\kappa_\eta(x) = \frac{1}{\eta}$. We set $\Delta x = \frac{2}{320}$ and compare the numerical solutions obtained with the Lax-Friedrich's scheme, and with Godunov's scheme, and for the non-oscillatory central scheme, we use a generalized slope limiter (8) with $\theta = 2$.

For the initial condition $\rho_0(x)$, two different functions are used. The first is a smooth function:

$$\rho_0(x) = 0.5 + 0.4\sin(\pi x). \tag{17}$$

The discontinuous one is:

$$\rho_0(x) = \begin{cases} 0.6, & \text{if } 1/3 < x < 2/3 \\ 0.2, & \text{otherwise.} \end{cases} \tag{18}$$

By now, the results displayed in Fig. 1, Fig. 2 are compared with respect to the reference solution, which was obtained from Godunov-type's scheme and

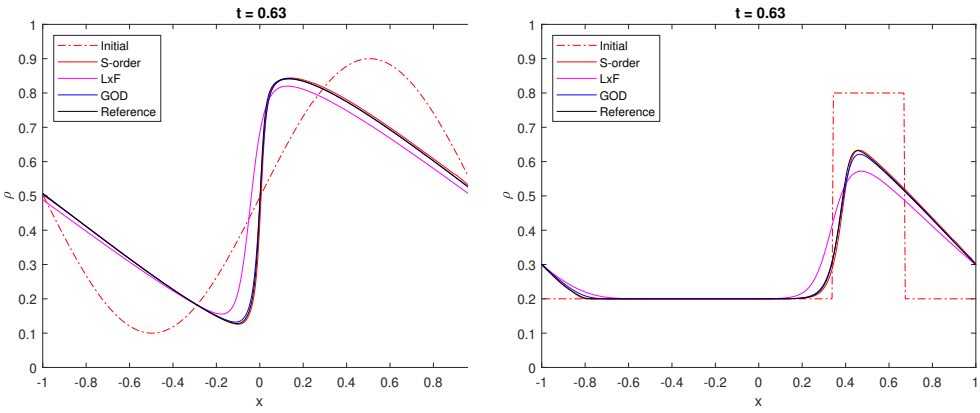

Figure 1: The solution to (1) with $\kappa_\eta(x) = \frac{2}{\eta}(1 - \frac{x}{\eta})$, (17) and (18). We compare solutions computed with second-order central scheme, Lax-Friedrich's scheme, and Godunov's scheme using $\Delta x = \frac{2}{320}$. Reference solution is computed with Godunov-type method with: $\Delta x = \frac{2}{320}$.

$\Delta x = \frac{2}{1280}$. In Fig. 1, Fig. 2 we observe that the central non-oscillatory scheme is much more accurate than the first order Lax-Friedrich-type's scheme.

We also estimate the L^1-errors at the final time, $T = 0.31$ to be:

$$e(\Delta x) = \frac{\Delta x}{2} \sum_{j=1}^{m} |\rho_{\Delta x}(T, x_j) - \rho_{\frac{\Delta x}{2}}(T, x_j)|,$$

$\rho_{\Delta x}$ is considered the numerical solution with space discretization equal to Δx in x_j. The results are given for decreasing kernel function in Table 1.

Test 2: We also seek to numerically investigate the convergence of the approximate solutions constructed by the proposed scheme to the solution of the classical local model (LWR),

$$\partial_t \rho + \partial_x(\rho(1 - \rho)) = 0, \quad x \in \mathbb{R},\ t > 0, \tag{19}$$

We compute convergence orders and L^1-errors of the non-local solution $\rho_{\Delta x}$ with scheme (16), $\theta = 2$, for $\eta \to 0$, with respect to the local solution ρ_L computed with the classic Lax-Friedrich method as reference solution, as follows:

$$e(\eta) = \|\rho_\eta(T, .) - \rho_L(T, .)\|_{L^1},$$

and

$$\gamma(\eta) = \log_2 \left(\frac{e(\eta)}{e(\frac{\eta}{2})} \right).$$

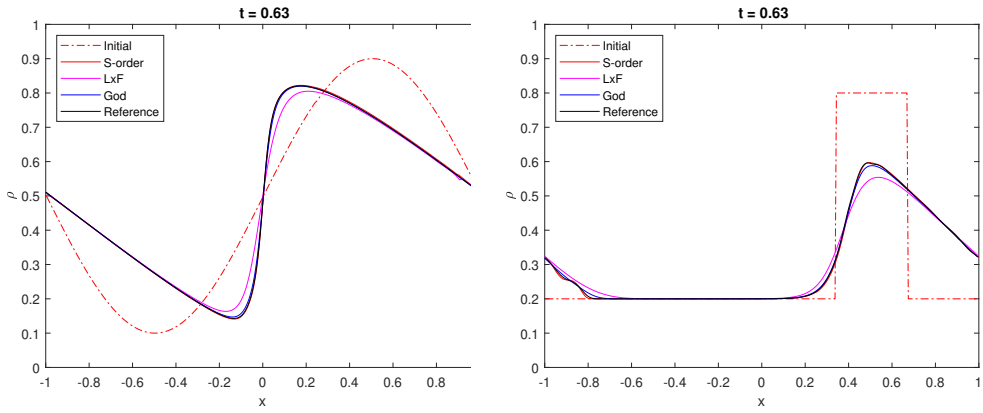

Figure 2: The solution to (1) with $\kappa_\eta(x) = \frac{1}{\eta}$, (17) and (18). We compare solutions computed with second-order-central scheme, Lax-Friedrich's scheme, and Godunov's scheme using $\Delta x = \frac{2}{320}$. Reference solution is computed with Godunov-type method with: $\Delta x = \frac{2}{320}$.

Table 1: Convergence orders and L^1_{error} for linear decreasing kernel $\kappa_\eta(x) = \frac{2}{\eta}(1 - \frac{x}{\eta})$ with linear velocity $v(\rho) = 1 - \rho$ at final time $T = 0.31$ corresponding to the initial data (17).

Δx	LxF	$\gamma(\Delta x)$	God	$\gamma(\Delta x)$	SCS	$\gamma(\Delta x)$
0.05	9.74E-02	-	2.72E-02	-	7.82E-04	-
0.025	4.94E-02	0.98	1.49E-02	0.86	1.92E-04	2.02
0.0125	2.49E-02	0.99	7E-03	1.08	4.75E-05	2.01
0.00625	1.26E-02	0.98	3.5E-03	1.00	1.21E-05	1.96
0.003125	6.3E-03	1.00	1.8E-03	0.95	2.96E-06	2.03

5. Conclusion

In this paper, we propose second-order numerical approximations that are of use to the solutions of non-local conservation laws in a one-dimensional space, motivated by their application to traffic flow with non-local mean downstream velocity. We use piecewise linear reconstruction in each cell to evaluate the convolution term in order to obtain the sought second-order accuracy. The results of several simulations demonstrate that Godunov's schemes are naturally

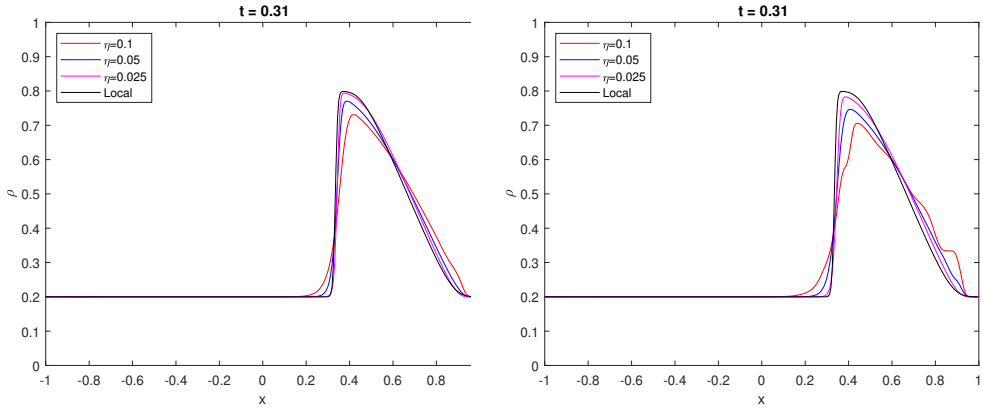

Figure 3: Density profile with $\kappa_\eta(x) = \frac{2}{\eta}(1 - \frac{x}{\eta})$ (left) and $\kappa_\eta(x) = \frac{1}{\eta}$ (right) for the non-local equation (1) with $\theta = 2$ and the local aquation (19). We can observe that the non-local solution $\rho_{\Delta x}$ with scheme (16) tends to the solution of (19)

Table 2: Convergence orders and L^1_{error} for $\eta \longrightarrow 0$. The data are related to the cases in Figure 3, with linear velocity $v(\rho) = 1 - \rho$ at time $T = 0.31$, corresponding to the initial datum (18). We remark that in case of linear decreasing kernel the L^1_{error} is smaller than the constant kernel.

	$\kappa_\eta = \frac{1}{\eta}$		$\kappa_\eta = \frac{1}{\eta}(1 - \frac{x}{\eta})$	
η	$\gamma(\eta)$	L^1_{error}	$\gamma(\eta)$	L^1_{error}
0.1	-	9.21E-02	-	6.55E-02
0.05	0.88	4.97E-02	0.9	3.5E-02
0.025	0.94	2.59E-02	0.89	1.88E-02

more accurate, but they are time-consuming. While the proposed scheme does significantly reduce numerical oscillation and shows substantial improvements with respect to Lax-Friedrich's scheme, it is in good agreement with the results obtained with Godunov's scheme.

Acknowledgements

This research was supported by the Lab of Applied Mathematics and Information systems (MASI). We want to thank Professor Jaouad Radouani for his help in this work.

References

[1] A. Aggarwal, R. M. Colombo, P. Goatin, Nonlocal systems of conservation laws in several space dimensions, *SIAM J. Numer. Anal.*, **53**, No 2 (2015), 963-983.

[2] P. Amorim, R. Colombo, A. Teixeira, On the numerical integration of scalar nonlocal conservation laws, *ESAIM M2AN*, **49**, No 1 (2015), 19-37.

[3] F. Betancourt, R. Burger, K. H. Karlsen, E. M. Tory, On nonlocal conservation laws modelling sedimentation. *Nonlinearity*, **24**, No 3 (2011), 855-885.

[4] S. Blandin, P. Goatin, Well-posedness of a conservation law with non-local flux arising in traffic flow modeling, *Numer. Math.*, **132**, No 2 (2016), 217-241.

[5] J. A. Carrillo, S. Martin, M.T. Wolfram, An improved version of the Hughes model for pedestrian flow, *Math. Models Methods Appl. Sci.*, **26**, No 4 (2016), 671-697.

[6] F. A. Chiarello, P. Goatin, Global entropy weak solutions for general non-local traffic flow models with anisotropic kernel, *ESAIM: M2AN*; doi:10.1051/m2an/2017066.

[7] R. M. Colombo, M. Garavello, M. Lecureux-Mercier, A class of nonlocal models for pedestrian traffic, *Math. Models Methods Appl. Sci.*, **22**, No 4 (2012), 1150023.

[8] R. M. Colombo, F. Marcellini, Nonlocal systems of balance laws in several space dimensions with applications to laser technology, *J. Differential Equations*, **259**, No 11 (2015), 6749-6773.

[9] R. Eymard, T. Gallouet, R. Herbin, Finite volume methods, *Handbook Numer. Anal.*, **7** (2000), 713-1018.

[10] J. Friedrich, O. Kolb, S. Gottlich, A Godunov type scheme for a class of LWR traffic flow models with non-local flux, *Netw. Heterog. Media.*, **13**, No 4 (2018), 531-547.

[11] P. Goatin, S. Scialanga, Well-posedness and finite volume approximations of the LWR traffic flow model with non-local velocity, *Netw. Heterog. Media.*, **11**, No 1 (2016), 107-121.

[12] E. Godlewski, P.A. Raviart, *Hyperbolic Systems of Conservation Laws*, Ellipses (1991).

[13] S. Gottlieb, D. I. Ketcheson, C. W. Shu, High order strong stability preserving time discretizations, *J. Sci. Comput.*, **38**, No 3 (2009), 251-289.

[14] R. M. Colombo, M. Herty, M. Mercier, Control of the continuity equation with a non local flow, *ESAIM Control Optim. Calc. Var.*, **17**, No 2 (2011), 353-379.

[15] M. Gugat, A. Keimer, G. Leugering, Z. Wang, Analysis of a system of nonlocal conservation laws for multi-commodity flow on networks, *Netw. Heterog. Media.*, **10**, No 4 (2015), 749-785.

[16] A. Kurganov, A. Polizzi, Non-oscillatory central schemes for a traffic flow model with Arrehenius look-ahead dynamics, *Netw. Heterog. Media.*, **4**, No 3 (2009), 431-451.

[17] H. Nessyahu, E. Tadmor, Non-oscillatory central differencing for hyperbolic conservation laws, *J. Comput. Phys.*, **87** (1990), 408-463.